Chasing the Two-Higgs-Doublet Model via Electroweak Corrections at e^+e^- Colliders

Pia Bredt,[1] Tatsuya Banno,[2] Marius Höfer,[3] Syuhei Iguro,[4,5] Wolfgang Kilian,[1] Yang Ma,[6] Jürgen Reuter,[7] and Hantian Zhang[8,*]

[1]*Center for Particle Physics Siegen, University of Siegen, Walter-Flex-Str. 3, 57072 Siegen, Germany*
[2]*Department of Physics, Nagoya University, Nagoya 464-8602, Japan*
[3]*Institute for Theoretical Physics, Karlsruhe Institute of Technology, Wolfgang-Gaede-Str. 1, 76131 Karlsruhe, Germany*
[4]*Institute for Advanced Research, Nagoya University, Nagoya 464–8601, Japan*
[5]*Kobayashi-Maskawa Institute for the Origin of Particles and the Universe, Nagoya University, Nagoya 464–8602, Japan*
[6]*Center for Cosmology, Particle Physics and Phenomenology, UCLouvain, B-1348 Louvain-la-Neuve, Belgium*
[7]*Deutsches Elektronen-Synchrotron DESY, Notkestr. 85, 22607 Hamburg, Germany*
[8]*Theoretical Physics Department, CERN, 1211 Geneva 23, Switzerland*

(Received 23 September 2025; accepted 29 January 2026; published 24 February 2026)

We present a comprehensive study of Higgs boson production associated with a neutrino pair at e^+e^- colliders ($e^+e^- \to h\nu\bar{\nu}$) at next-to-leading-order accuracy in both the standard model and the two-Higgs-doublet model. We show that these new physics effects will be observable in total and differential cross sections when compared with theoretical predictions that include electroweak corrections, even in the Higgs alignment limit. This highlights the potential of precision studies at future e^+e^- colliders for searching new physics.

DOI: 10.1103/mnqp-l2h9

The Higgs boson discovered at the Large Hadron Collider (LHC) [1,2] has completed the particle content predicted by the standard model (SM) [3–5]. Despite its great success, fundamental problems such as the origins of baryon asymmetry of the universe and dark matter persist, necessitating new physics beyond the SM (BSM). In this context, precise studies of Higgs boson properties and direct searches of new physics form two complementary focuses in modern particle physics. Over the past decade, the accuracy of Higgs-sector measurements has been greatly improved at the LHC, while there is still room for new physics effects at the ten percent level [6,7]. Although the LHC is well suited for studying the gross picture of the Higgs sector, future e^+e^- colliders such as FCC-ee, CEPC, ILC/LCF, and CLIC [8–15] are required for the determination of Higgs boson properties at the electroweak scale with a few permille accuracy.

In this Letter, we show that there are realistic opportunities for searching new physics through the precision program at future high-energy e^+e^- colliders, particularly via electroweak (EW) corrections to scattering processes. We demonstrate this possibility through a comprehensive study of single Higgs production ($e^+e^- \to h + \nu_\ell\bar{\nu}_\ell$ with $\ell = e, \mu, \tau$) at next-to-leading-order (NLO) EW accuracy in both the SM and two-Higgs-doublet model (2HDM). The 2HDM is one of the simplest extensions of the SM and has rich phenomenology [16]. This model can resolve the vacuum metastability issue [17] and provide strong first-order electroweak phase transition for baryogenesis [18] and detectable gravitational waves [19]. It often appears as a low-energy scalar sector of more UV-complete theories, for example, the left-right symmetric models [20–22] and supersymmetric (SUSY) models [23,24]. In the 2HDM there exists an alignment limit in which the discovered Higgs boson behaves exactly as the SM one at the tree level. We show that even in this limit NLO EW corrections involving new particles can induce few percent effects with respect to the SM predictions, thereby offering an important window to access this model.

In the literature, the on-shell Higgsstrahlung process, $e^+e^- \to Zh$, has been intensively investigated. For example, full NLO EW corrections in the 2HDM and SUSY models are computed in Refs. [25–28], and the higher-order calculations in the SM for related triangle and box form factors are computed in Refs. [29–35]. However, the more complicated off-shell single Higgs production $e^+e^- \to h\nu\bar{\nu}$ is not so well studied. Pioneering works for this $2 \to 3$ process include the full NLO EW corrections in the SM [36–38] and one-loop triangle form factor corrections in the SUSY models [39–42], while a complete NLO EW study in BSM theories is still missing. This process is advantageous, since at higher center-of-mass energies, $\sqrt{s} = 365$ and 550 GeV, the cross section is roughly an

*Contact author: hantian.zhang@cern.ch

order of magnitude larger than those of $e^+e^- \to h\ell\overline{\ell}$ processes. In particular, the fact that its cross section at larger $\sqrt{s}$ is dominated by WW fusion allows an independent probe of new physics effects other than Zh production.

Regarding the 2HDM we follow the convention of Refs. [43–45]. The two Higgs doublets are denoted by Φ_1 and Φ_2, each acquiring a vacuum expectation value (VEV). If both doublets couple to fermions as in the SM, the neutral scalars induce large tree level flavor changing neutral currents (FCNCs) in general. To prevent such large FCNCs, it is useful to assign a $\mathbb{Z}_2$ symmetry charge [46,47]. As a result, there are four types of Yukawa structures depending on the $\mathbb{Z}_2$ charge assignment [48,49]. The CP-conserving Higgs potential is given by

$$\begin{aligned} V = {} & m_1^2\Phi_1^\dagger\Phi_1 + m_2^2\Phi_2^\dagger\Phi_2 - m_{12}^2(\Phi_1^\dagger\Phi_2 + \Phi_2^\dagger\Phi_1) \\ & + \frac{\lambda_1}{2}(\Phi_1^\dagger\Phi_1)^2 + \frac{\lambda_2}{2}(\Phi_2^\dagger\Phi_2)^2 + \frac{\lambda_3}{2}(\Phi_1^\dagger\Phi_1)(\Phi_2^\dagger\Phi_2) \\ & + \frac{\lambda_4}{2}(\Phi_1^\dagger\Phi_2)(\Phi_2^\dagger\Phi_1) + \frac{\lambda_5}{2}\left[(\Phi_1^\dagger\Phi_2)^2 + (\Phi_2^\dagger\Phi_1)^2\right], \end{aligned} \tag{1}$$

where the $\mathbb{Z}_2$ symmetry ($\Phi_1 \to -\Phi_1$ and $\Phi_2 \to \Phi_2$) is softly broken by the m_{12}^2 term. After spontaneous symmetry breaking, two mixing angles α and β can be introduced to obtain the mass eigenstates. In addition to the 125 GeV SM-like Higgs boson h, we have four scalars: charged scalars $H^\pm$, neutral scalar H, and pseudoscalar A. The parameter $c_{\beta\alpha} \equiv \cos(\beta-\alpha)$ governs the mixing between CP-even scalars h and H, while $t_\beta \equiv \tan(\beta)$ represents the ratio of two VEVs and determines the Yukawa couplings. Note that the Higgs alignment limit is realized in $c_{\beta\alpha} = 0$ such that h is aligned with the SM Higgs. Now the extended Higgs sector is parametrized by $c_{\beta\alpha}, t_\beta, \lambda_5, m_H, m_A, m_{H^\pm}$.

We perform a complete NLO EW calculation in the 2HDM for $e^+e^- \to h\nu\bar{\nu}$ by employing the automated NLO framework [50–54] of the multipurpose Monte-Carlo generator Whizard [55,56] with an interface to generic one-loop amplitude providers OpenLoops2 [57] and Recola [58,59] for the SM, and Recola2 [59] for the 2HDM. We note that OpenLoops2 supports the 2HDM at NLO QCD [60]. Representative 2HDM Feynman diagrams are shown in Fig. 1. For this Letter a massive electron-positron beam setup is used in Whizard, such that initial-state collinear singularities are regulated, while soft singularities are handled in an automated way within the Frixione-Kunszt-Signer subtraction [61]. In the SM case, we compare our NLO EW cross section with Ref. [37] and find agreement at the 0.2% level at $\sqrt{s} = 500$ GeV. The small residual discrepancy can be attributed to differences in the treatment of complex masses [38,57,62] and the structure function approach [63–65]. In the 2HDM case, electroweak renormalization schemes are developed in Refs. [45,66–68]. We employ two on-shell renormalization schemes defined in Ref. [45]. The default on-shell scheme for mixing angles in Recola2 serves as our reference scheme, while the background-field approach is used to estimate scheme uncertainties. λ_5 is renormalized in the $\overline{\text{MS}}$ scheme. We compare our NLO EW cross sections for $pp \to h\mu^+\nu_\mu$ in several 2HDM benchmarks in different renormalization schemes with Ref. [45] and HAWK [69], and we find excellent agreement at the permille level. This is one of the most extensive NLO applications of Whizard, not due to the complexity of this process, but because of the massive scan over parameter points performed for the same process as outlined below, capitalizing on the massive parallelization features of Whizard [70,71].

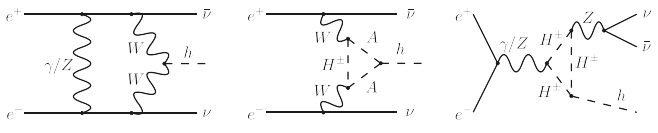

FIG. 1. Diagrams for $e^+e^- \to h\nu\bar{\nu}$ at NLO EW in 2HDM.

In the following benchmark, we compare predictions between the SM and type I 2HDM. The SM input parameters are $G_F = 1.166378 \times 10^{-5}$ GeV, $m_h = 125.2$ GeV, $m_Z = 91.1539$ GeV, $\Gamma_Z = 2.4946$ GeV, $m_W = 80.3407$ GeV, $\Gamma_W = 2.14$ GeV, $m_b = 4.183$ GeV, $m_t = 172.56$ GeV, $m_e = 5.110 \times 10^{-4}$ GeV, and the G_μ scheme is employed. The W and Z masses and widths are pole values, which are converted from measured on-shell values. Light quark and lepton mass effects are negligible for this process, except for the electron mass due to large logarithms from the initial-state radiation (ISR). A 2HDM benchmark point allowed by theoretical and experimental constraints based on HiggsTools [72] is $m_H = m_{H^\pm} = 400$ GeV, $m_A = 435$ GeV, $c_{\beta\alpha} = 0.03734$, $t_\beta = 1.88$, $\lambda_5 = -2.54$. The on-shell renormalization scheme for mixing angles is employed, and the renormalization scale for λ_5 is set to $\sqrt{s}$.

In Table I we present the LO and NLO EW total cross sections at $\sqrt{s} = 365$ and 550 GeV (both unpolarized) in the SM and the 2HDM benchmark, as well as in the alignment limit $c_{\beta\alpha} = 0$. At LO, increasing the energy from $\sqrt{s} = 365$ to 550 GeV enhances the cross section by about

TABLE I. Total cross sections for $e^+e^- \to h\nu\bar{\nu}$ in the SM and the type I 2HDM benchmark without cuts, and the alignment limit is realized with $\cos(\beta-\alpha) = 0$. The relative difference $(\sigma_{\text{2HDM}} - \sigma_{\text{SM}})/\sigma_{\text{SM}}$ is reported at LO and NLO. Monte Carlo integration errors larger than 0.01 fb are indicated in brackets.

	$\sqrt{s} = 365$ GeV		$\sqrt{s} = 550$ GeV	
	LO [fb]	NLO EW [fb]	LO [fb]	NLO EW [fb]
SM	55.79	52.44(1)	97.82(1)	88.45(2)
2HDM	55.71	51.45(1)	97.67(1)	86.59(2)
Relative difference	−0.1%	−1.9%	−0.2%	−2.1%
2HDM (aligned)	55.79	51.58(1)	97.81(1)	86.83(2)
Relative difference	0.0%	−1.7%	0.0%	−1.8%

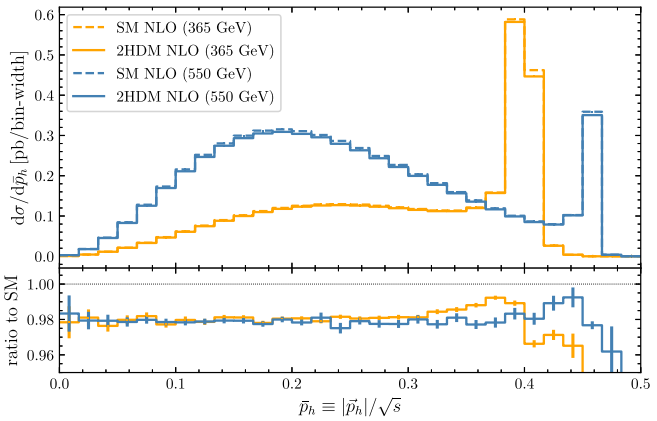

FIG. 2. Top panel: differential cross sections at NLO as a function of the normalized Higgs three-momentum $\bar{p}_h \equiv |\vec{p}_h|/\sqrt{s}$ at $\sqrt{s} = 365$ GeV (orange) and $\sqrt{s} = 550$ GeV (blue), in the SM (dashed) and 2HDM (solid). Bottom panel: ratios of the 2HDM predictions to the SM ones at NLO.

75%, both in the SM and the 2HDM. For both energies, we find only a permille level reduction of the cross section in the 2HDM compared to the SM, which vanishes in the alignment limit. The situation changes at NLO: while the EW corrections are negative in all cases at the order of ten percent, they are more pronounced in the 2HDM, even in the alignment limit. Specifically, the reduction amounts to 1.7% (1.8%) and 1.9% (2.1%) at $\sqrt{s} = 365$ (550) GeV when comparing the 2HDM cross sections, with and without alignment, to the SM. Therefore, we conclude that NLO EW corrections are a very sensitive probe of BSM effects in our 2HDM benchmarks.

In Fig. 2 we show the differential cross section as a function of the normalized three-momentum of the Higgs, $\bar{p}_h \equiv |\vec{p}_h|/\sqrt{s}$, again for two energies $\sqrt{s} = 365$ and 550 GeV. We focus on the comparison between the SM and 2HDM at NLO. In the upper panel, for $\sqrt{s} = 365(550)$ GeV the peak corresponding to on-shell Zh production, with the Z subsequently decaying into $\nu\bar{\nu}$, is located at $\bar{p}_h \approx 0.401$ (0.459), and values up to $\bar{p}_h \approx 0.441$ (0.474) are kinematically allowed. Most of the cross section comes from the broader WW-fusion contribution at lower values of $\bar{p}_h$. We observe that the relative contribution from the Zh channel decreases when going to higher $\sqrt{s}$. In the lower panel we show the ratios of the 2HDM predictions to those in the SM. Both for $\sqrt{s} = 365$ and 550 GeV we observe that the 2HDM effects lead to an overall reduction of the cross sections by about 2%, in line with the findings for the total cross sections in Table I. For most of the $\bar{p}_h$ range the shift is flat, becoming smaller just below the Zh peak, but larger once crossing to higher $\bar{p}_h$. The separation of WW and Zh channels in the differential distribution enables simultaneous probes of 2HDM effects in a single process. This separation could be achieved, for example, through a cut on the energy of the Higgs boson and further facilitated by the use of polarized beams, which is beyond the scope of this Letter.

Moreover, at $\sqrt{s} = 240$ GeV we find a similar 2% reduction relative to the SM prediction (43.87 fb) at NLO. Nevertheless, the ISR effects beyond NLO can reach several percent around 240 GeV [37], due to the kinematical effect near the Zh production threshold, we therefore focus on $\sqrt{s} = 365$ and 550 GeV cases. At larger $\sqrt{s}$, our process is dominated by the WW-fusion channel and away from the threshold region of Zh production, thus the beyond NLO ISR effects are only at the few permille level [37]. We note that the NLO ISR effects are consistently taken into account in our calculation through the real corrections. We also investigate the Zh-mediated process $e^+e^- \to h\mu^+\mu^-$ and find much smaller cross sections of 4.04(1.72) fb at $\sqrt{s} = 365(550)$ GeV. Hence, the process $e^+e^- \to h\nu\bar{\nu}$ is advantageous in probing new physics due to large WW-fusion contributions.

We emphasize that this indirect probe at future e^+e^- colliders complements direct searches for 2HDM. At the (HL)-LHC, single production of an additional scalar via gauge interaction is suppressed by the h-H mixing, whereas production through Yukawa interaction is highly model dependent. Although electroweak pair production of additional scalars, e.g., $pp \to W^+ \to H^+H$ is not suppressed by the mixing, the production rates decrease rapidly with increasing scalar masses. While at e^+e^- colliders, if the collision energy is sufficiently high, e.g., in the benchmark with $\sqrt{s} = 550$ GeV and $m_H = 400$ GeV, the process $e^+e^- \to Z^* \to ZH$ becomes accessible, its cross section remains suppressed by the mixing and vanishes in the alignment limit. In contrast, for $e^+e^- \to h\nu\bar{\nu}$ we show that the difference in cross sections between the 2HDM and the SM at NLO EW can be sizable even in the alignment limit, thereby providing an important complementary window to probe the model.

In the next stage, we present a comprehensive analysis for four types of $\mathbb{Z}_2$-symmetric 2HDMs: type I, II, X (lepton specific), and Y (flipped). We generate the parameter points with ScannerS [73,74] and HiggsTools [72] based on HiggsBounds [75–78] and HiggsSignals [79,80] to take theoretical and experimental constraints into account. For instance, these constraints include tree-level perturbative unitarity, boundedness from below and electroweak vacuum stability as theoretical constraints, and electroweak precision observables, flavor-changing processes, direct searches at the LHC and LEP as experimental constraints. In our setup, the additional scalars are degenerate. The free parameters $m_\phi \equiv m_H = m_A = m_{H^\pm}$, $c_{\beta\alpha}$, t_β, and λ_5 are chosen from the 95% confidence level (CL) allowed region. In total, we generate 30 000 parameter points for the type I, II, and Y, and 70 000 parameter points for the type X.

In our sensitivity analysis, the 2HDM predictions in parameter planes of $c_{\beta\alpha}$, λ_5, t_β, $c_\alpha/s_\beta \equiv \cos(\alpha)/\sin(\beta)$, m_ϕ are presented in Figs. 3 and 4 at $\sqrt{s} = 365$ GeV, and in

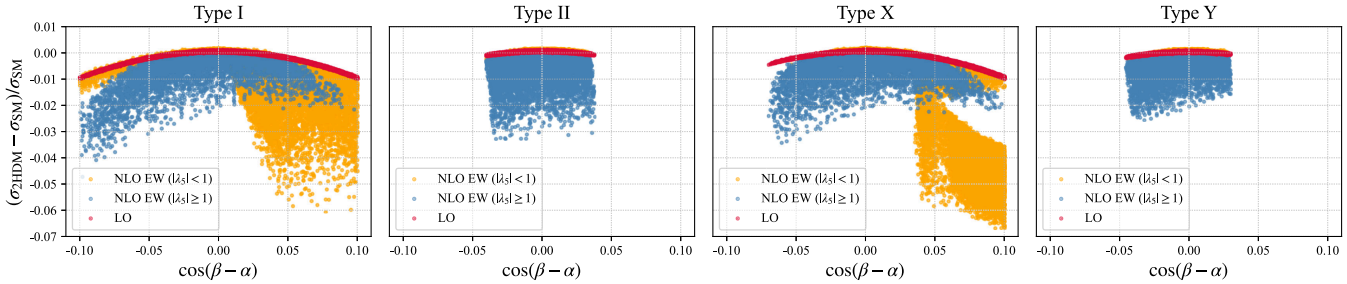

FIG. 3. Type I, II, X, and Y 2HDM predictions in the $\cos(\beta-\alpha)$ plane at $\sqrt{s}=365$ GeV within the allowed parameter space, with $|\cos(\beta-\alpha)|<0.1$. Relative differences with respect to the SM are shown at LO (red) and NLO (orange for $|\lambda_5|<1$, blue for $|\lambda_5|\geq 1$). The combined theoretical and experimental uncertainty is estimated to be 0.92%.

Fig. 5 for $\sqrt{s}=550$ GeV. The relative differences $(\sigma_{2HDM}-\sigma_{SM})/\sigma_{SM}$ at LO and NLO are shown for $|c_{\beta\alpha}|<0.1$, covering more than the estimated 95% CL allowed range for the least constrained type I 2HDM at future e^+e^- colliders [81,82]. To estimate the theoretical uncertainty, we compute the renormalization scheme dependence for mixing angles in the type I 2HDM for hundreds of parameter points, finding the maximal uncertainty of 0.7%(0.8%) for the relative difference at $\sqrt{s}=365(550)$ GeV for $|c_{\beta\alpha}|<0.1$. We note that NNLO mixed QCD-EW SM corrections yield only few permille effects in the G_μ scheme [31,34], and that in the relative difference, higher-order SM corrections cancel and do not contribute to the uncertainty. To further reduce the scheme uncertainty, NNLO EW corrections in the 2HDM would be required. On the other hand, the experimental uncertainty of the cross section measurement will reach 0.6%(0.3%) at $\sqrt{s}=365(500)$ GeV with 4.3(6.4) ab^{-1} of data [13]. Therefore, the potential gain from an NNLO-level theoretical uncertainty reduction would not affect our conclusion below. We expect that the sensitivity difference between $\sqrt{s}=500$ and 550 GeV is negligible.

It is shown in Fig. 3 that $c_{\beta\alpha}$ is the key parameter governing the LO 2HDM deviation from the SM. We first discuss the type I 2HDM plot at $\sqrt{s}=365$ GeV. The LO relative difference (red) vanishes as the $|c_{\beta\alpha}|$ approaches the alignment limit and increases with $|c_{\beta\alpha}|$ reaching at most -1%. At NLO, however, richer phenomena arise that cannot be described by a single parameter. We highlight the impact of the NLO EW corrections by showing two branches separating cases of small $|\lambda_5|<1$ (orange) and large $|\lambda_5|\geq 1$ (blue). The NLO relative difference reaches -6% in the small-$|\lambda_5|$ branch and -4% in the large-$|\lambda_5|$ branch. The -2% deviation in the alignment limit is observed in the large-$|\lambda_5|$ branch, however, it does not imply that this effect is solely driven by the λ_5 self-interaction, since Fig. 4 indicates sizable mass effects and top-Yukawa corrections deviating from the SM when $c_\alpha/s_\beta\neq 1$. Note that the ratio c_α/s_β governs the top-Yukawa coupling to the Higgs in the same way across all four 2HDM types [83]. We find that the relative difference at $\sqrt{s}=550$ GeV in Fig. 5 is similar to $\sqrt{s}=365$ GeV but slightly more pronounced. Since the expected accuracy of the cross section measurement will be better at higher energies, we conclude that the operation at 550 GeV will be more sensitive to the 2HDM effects. For the remaining plots in Fig. 3, the relative differences reach about -7% in the type X, and around -3% in the more constrained type II and Y. We note that although our NLO predictions for Higgs production are insensitive to different 2HDM Yukawa structures, the allowed parameter space across types determines the shapes of distributions, providing a restricted ability to discriminate between 2HDM types. To further distinguish them, we need to include Higgs decay channels. We note that since both the beyond NLO ISR effects and the NNLO mixed QCD-EW corrections are at the few permille level, the discrimination

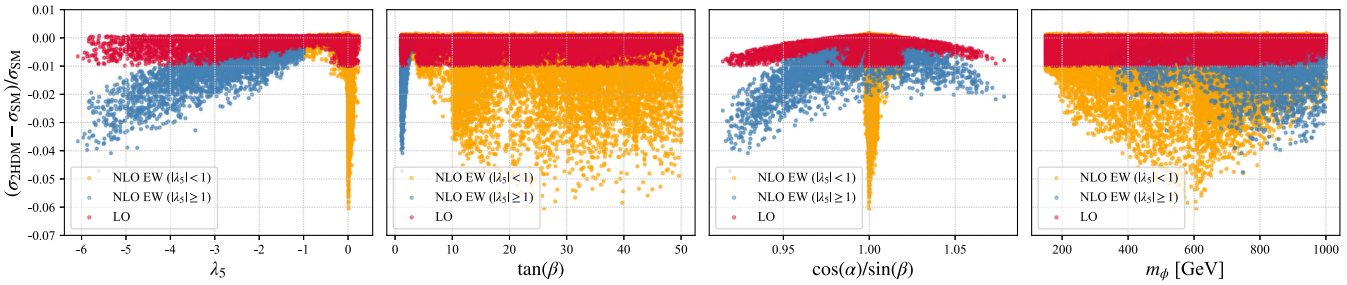

FIG. 4. Type I 2HDM predictions in the λ_5, $\tan(\beta)$, $\cos(\alpha)/\sin(\beta)$ and m_ϕ parameter planes at $\sqrt{s}=365$ GeV within the allowed parameter space, with $|\cos(\beta-\alpha)|<0.1$.

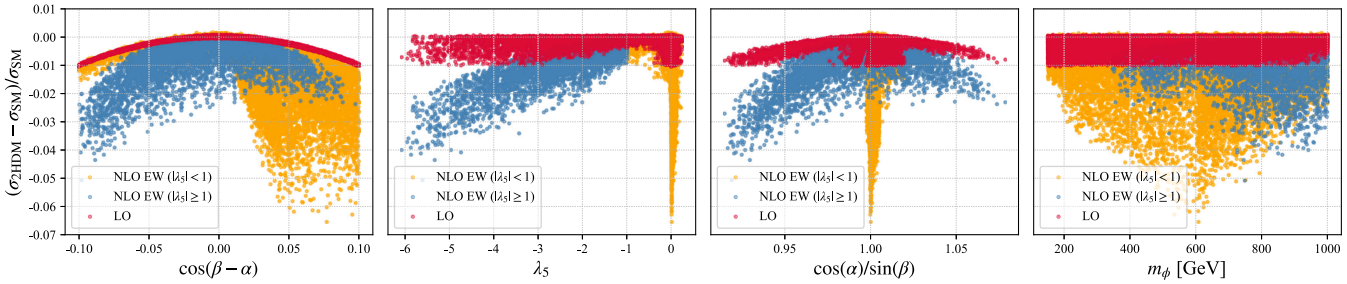

FIG. 5. Type I 2HDM predictions at $\sqrt{s} = 550$ GeV within the allowed parameter space, with $|\cos(\beta - \alpha)| < 0.1$. The combined theoretical and experimental uncertainties are estimated to be 0.85%.

between the SM and the 2HDMs observed at NLO EW is valid even without a full NNLO calculation.

To scrutinize the NLO effects, the relative differences in other parameter planes at $\sqrt{s} = 365$ GeV are shown in Fig. 4 for the type I 2HDM. Although the large-$|\lambda_5|$ branch naturally develops sizable effects, the small-$|\lambda_5|$ branch localized near $\lambda_5 \approx 0$ and $c_\alpha/s_\beta \approx 1$, yet spread across m_ϕ from 200 GeV to 1 TeV, is particularly interesting. This implies that these large deviations are genuine NLO effects, with mixing angles and m_ϕ all playing a role. In addition, there is no clear correlation between the NLO effects and the parameters t_β and m_ϕ. This phenomenon cannot be easily parameterized within an effective field theory approach, highlighting the importance of NLO calculations in UV-complete BSM theories.

In summary, we conduct the first full NLO EW study of Higgs production $e^+e^- \to h\nu\bar{\nu}$ in all four types of $\mathbb{Z}_2$-symmetric 2HDMs, over a vast allowed parameter space. We find that the 2HDM effects are significantly enhanced at NLO, with deviations from the SM predictions reaching -6% to -7% with $|c_{\beta\alpha}| < 0.1$ for $\sqrt{s} = 365$ and 550 GeV. Even in the Higgs alignment limit, these deviations can reach -2% to -3%, making them experimentally observable. We emphasize that this discrimination power between the SM and 2HDMs arises only at NLO, but is absent at LO. We show that the differential distributions disentangle the WW-fusion and Zh channels, allowing simultaneous new physics probes. In a broader context of precision physics at future e^+e^- colliders, our findings underscore the crucial importance of higher-order electroweak calculations in UV-complete BSM theories for new physics searches, opening up new windows that are complementary to the LHC searches.

Acknowledgments—We thank Georg Weiglein, Johannes Braathen, and Jean-Nicolas Lang for useful discussions, and thank Matthias Steinhauser and Gudrun Heinrich for useful comments on the manuscript. H. Z. is funded by the European Union under the Marie Skłodowska-Curie Actions (MSCA) Grant No. 101202083—"HINOVA," and by the Swiss National Science Foundation (SNSF) Grant No. TMSGI2 211209. P. B., M. H., and W. K. are supported by the Deutsche Forschungsgemeinschaft (DFG, German Research Foundation) under Grant No. 396021762—TRR 257 "Particle Physics Phenomenology after the Higgs Discovery." J. R. is supported by the DFG under the German Excellence Strategy-EXC 2121 "Quantum Universe"-390833306, and the National Science Centre (Poland) under OPUS research Project No. 2021/43/B/ST2/01778. Y. M. is supported by a Postdoctoral Fellowship of the Fond de la Recherche Scientifique de Belgique (F.R.S.-FNRS), Belgium, and the IISN convention 4.4517.08 "Theory of fundamental interactions." T. B. is supported by the JST SPRING Grant No. JPMJSP2125. S. I. is supported by the JSPS KAKENHI Grants No. 22K21347, No. 24K22879, No. 24K23939, No. 25K17385, No. JPJSCCA20200002, and the Toyoaki scholarship foundation. S. I. and H. Z. also thank the Paul Scherrer Institute and the University of Zurich for their hospitality during the course of this project.

Data availability—The data that support the findings of this article are not publicly available. The data are available from the authors upon reasonable request.

[1] G. Aad *et al.* (ATLAS Collaboration), Observation of a new particle in the search for the standard model Higgs boson with the ATLAS detector at the LHC, Phys. Lett. B **716**, 1 (2012).
[2] S. Chatrchyan *et al.* (CMS Collaboration), Observation of a new boson at a mass of 125 GeV with the CMS experiment at the LHC, Phys. Lett. B **716**, 30 (2012).
[3] S. L. Glashow, Partial symmetries of weak interactions, Nucl. Phys. **22**, 579 (1961).
[4] S. Weinberg, A model of leptons, Phys. Rev. Lett. **19**, 1264 (1967).
[5] A. Salam, Weak and electromagnetic interactions, Conf. Proc. C **680519**, 367 (1968).
[6] A. Tumasyan *et al.* (CMS Collaboration), A portrait of the Higgs boson by the CMS experiment ten years after the discovery, Nature (London) **607**, 60 (2022); **623**, E4 (2023).
[7] G. Aad *et al.* (ATLAS Collaboration), A detailed map of Higgs boson interactions by the ATLAS experiment ten years after the discovery, Nature (London) **607**, 52 (2022); **612**, E24 (2022).

[8] A. Abada *et al.* (FCC Collaboration), FCC physics opportunities: Future circular collider conceptual design report volume 1, Eur. Phys. J. C **79**, 474 (2019).

[9] M. Benedikt *et al.* (FCC Collaboration), Future circular collider feasibility study report: Volume 1, physics, experiments, detectors, Eur. Phys. J. C **85**, 1468 (2025).

[10] M. Dong *et al.* (CEPC Study Group), CEPC conceptual design report: Volume 2—physics & detector, arXiv:1811.10545.

[11] W. Abdallah *et al.* (CEPC Study Group), CEPC technical design report: Accelerator, Radiat. Detect. Technol. Methods **8**, 1 (2024); **9**, 184(E) (2025).

[12] A. Aryshev *et al.* (ILC International Development Team), The international linear collider: Report to Snowmass 2021, arXiv:2203.07622.

[13] D. Attié *et al.* (Linear Collider Vision Collaboration), A linear collider vision for the future of particle physics, arXiv:2503.19983.

[14] L. Linssen, A. Miyamoto, M. Stanitzki, and H. Weerts, Physics and detectors at CLIC: CLIC conceptual design report, arXiv:1202.5940.

[15] E. Adli *et al.*, The compact linear e^+e^- collider (CLIC), arXiv:2503.24168.

[16] T. D. Lee, A theory of spontaneous T violation, Phys. Rev. D **8**, 1226 (1973).

[17] M. Sher, Electroweak Higgs potentials and vacuum stability, Phys. Rep. **179**, 273 (1989).

[18] A. G. Cohen, D. B. Kaplan, and A. E. Nelson, Progress in electroweak baryogenesis, Annu. Rev. Nucl. Part. Sci. **43**, 27 (1993).

[19] G. C. Dorsch, S. J. Huber, T. Konstandin, and J. M. No, A second Higgs doublet in the early universe: Baryogenesis and gravitational waves, J. Cosmol. Astropart. Phys. 05 (2017) 052.

[20] J. C. Pati and A. Salam, Lepton number as the fourth color, Phys. Rev. D **10**, 275 (1974); **11**, 703(E) (1975).

[21] R. N. Mohapatra and J. C. Pati, Left-right gauge symmetry and an isoconjugate model of CP violation, Phys. Rev. D **11**, 566 (1975).

[22] G. Senjanovic and R. N. Mohapatra, Exact left-right symmetry and spontaneous violation of parity, Phys. Rev. D **12**, 1502 (1975).

[23] P. Fayet, Spontaneously broken supersymmetric theories of weak, electromagnetic and strong interactions, Phys. Lett. B **69**, 489 (1977).

[24] S. P. Martin, A supersymmetry primer, Adv. Ser. Dir. High Energy Phys. **18**, 1 (1998).

[25] W. Xie, R. Benbrik, A. Habjia, S. Taj, B. Gong, and Q.-S. Yan, Signature of 2HDM at Higgs factories, Phys. Rev. D **103**, 095030 (2021).

[26] M. Aiko, S. Kanemura, and K. Mawatari, Next-to-leading-order corrections to the Higgs strahlung process from electron–positron collisions in extended Higgs models, Eur. Phys. J. C **81**, 1000 (2021).

[27] Anisha, F. Arco, S. Di Noi, C. Englert, and M. Mühlleitner, Z and Higgs factory implications of two Higgs doublets with first-order phase transitions, J. High Energy Phys. 10 (2025) 179.

[28] S. Heinemeyer, S. Paßehr, and C. Schappacher, Light neutral Higgs-boson production at e^+e^- colliders in the complex MSSM and NMSSM: A full one-loop analysis, arXiv:2507.00931.

[29] B. A. Kniehl and M. Steinhauser, Three loop $O(\alpha_s^2 G_F M_t^2)$ corrections to Higgs production and decay at e^+e^- colliders, Nucl. Phys. **B454**, 485 (1995).

[30] Y. Gong, Z. Li, X. Xu, L. L. Yang, and X. Zhao, Mixed QCD-EW corrections for Higgs boson production at e^+e^- colliders, Phys. Rev. D **95**, 093003 (2017).

[31] Q.-F. Sun, F. Feng, Y. Jia, and W.-L. Sang, Mixed electroweak-QCD corrections to $e^+e^- \to HZ$ at Higgs factories, Phys. Rev. D **96**, 051301 (2017).

[32] Y. Wang, X. Xu, and L. L. Yang, Two-loop triangle integrals with 4 scales for the HZV vertex, Phys. Rev. D **100**, 071502 (2019).

[33] C. Ma, Y. Wang, X. Xu, L. L. Yang, and B. Zhou, Mixed QCD-EW corrections for Higgs leptonic decay via HW^+W^- vertex, J. High Energy Phys. 09 (2021) 114.

[34] Y. Wang, L. L. Yang, and B. Zhou, FastGPL: A C++ library for fast evaluation of generalized polylogarithms, arXiv:2112.04122.

[35] A. Freitas and Q. Song, Two-loop electroweak corrections with fermion loops to $e^+e^- \to ZH$, Phys. Rev. Lett. **130**, 031801 (2023).

[36] G. Belanger, F. Boudjema, J. Fujimoto, T. Ishikawa, T. Kaneko, K. Kato, and Y. Shimizu, Full one loop electroweak radiative corrections to single Higgs production in e^+e^-, Phys. Lett. B **559**, 252 (2003).

[37] A. Denner, S. Dittmaier, M. Roth, and M. M. Weber, Electroweak radiative corrections to single Higgs boson production in e^+e^- annihilation, Phys. Lett. B **560**, 196 (2003).

[38] A. Denner, S. Dittmaier, M. Roth, and M. M. Weber, Electroweak radiative corrections to $e^+e^- \to \nu\bar{\nu}H$, Nucl. Phys. **B660**, 289 (2003).

[39] H. Eberl, W. Majerotto, and V. C. Spanos, Radiative corrections to single Higgs boson production in e^+e^- annihilation, Phys. Lett. B **538**, 353 (2002).

[40] H. Eberl, W. Majerotto, and V. C. Spanos, Single Higgs boson production at future linear colliders including radiative corrections, Nucl. Phys. **B657**, 378 (2003).

[41] T. Hahn, S. Heinemeyer, and G. Weiglein, MSSM Higgs boson production at the linear collider: Dominant corrections to the WW fusion channel, Nucl. Phys. **B652**, 229 (2003).

[42] F. Wang, W. Wang, F.-q. Xu, J. M. Yang, and H. Zhang, Virtual effects of split SUSY in Higgs productions at linear colliders, Eur. Phys. J. C **51**, 713 (2007).

[43] M. Aoki, S. Kanemura, K. Tsumura, and K. Yagyu, Models of Yukawa interaction in the two Higgs doublet model, and their collider phenomenology, Phys. Rev. D **80**, 015017 (2009).

[44] A. Denner, J.-N. Lang, and S. Uccirati, NLO electroweak corrections in extended Higgs sectors with Recola2, J. High Energy Phys. 07 (2017) 087.

[45] A. Denner, S. Dittmaier, and J.-N. Lang, Renormalization of mixing angles, J. High Energy Phys. 11 (2018) 104.

[46] E. A. Paschos, Diagonal neutral currents, Phys. Rev. D **15**, 1966 (1977).

[47] S. L. Glashow and S. Weinberg, Natural conservation laws for neutral currents, Phys. Rev. D **15**, 1958 (1977).

[48] V. D. Barger, J. L. Hewett, and R. J. N. Phillips, New constraints on the charged Higgs sector in two Higgs doublet models, Phys. Rev. D **41**, 3421 (1990).

[49] Y. Grossman, Phenomenology of models with more than two Higgs doublets, Nucl. Phys. **B426**, 355 (1994).

[50] P. M. Bredt, W. Kilian, J. Reuter, and P. Stienemeier, NLO electroweak corrections to multi-boson processes at a muon collider, J. High Energy Phys. 12 (2022) 138.

[51] F. Bach, B. C. Nejad, A. Hoang, W. Kilian, J. Reuter, M. Stahlhofen, T. Teubner, and C. Weiss, Fully-differential top-pair production at a lepton collider: From threshold to continuum, J. High Energy Phys. 03 (2018) 184.

[52] B. Chokoufé Nejad, W. Kilian, J. M. Lindert, S. Pozzorini, J. Reuter, and C. Weiss, NLO QCD predictions for off-shell $t\bar{t}$ and $t\bar{t}H$ production and decay at a linear collider, J. High Energy Phys. 12 (2016) 075.

[53] J. Kalinowski, W. Kilian, J. Reuter, T. Robens, and K. Rolbiecki, Pinning down the invisible sneutrino at the ILC, in *International Linear Collider Workshop (LCWS08 and ILC08)* (2009), arXiv:0901.4700.

[54] T. Robens, J. Kalinowski, K. Rolbiecki, W. Kilian, and J. Reuter, (N)LO simulation of chargino production and decay, Acta Phys. Pol. B **39**, 1705 (2008), https://www.actaphys.uj.edu.pl/R/39/7/1705.

[55] W. Kilian, T. Ohl, and J. Reuter, Whizard: Simulating multi-particle processes at LHC and ILC, Eur. Phys. J. C **71**, 1742 (2011).

[56] M. Moretti, T. Ohl, and J. Reuter, O'Mega: An optimizing matrix element generator, arXiv:hep-ph/0102195.

[57] F. Buccioni, J.-N. Lang, J. M. Lindert, P. Maierhöfer, S. Pozzorini, H. Zhang, and M. F. Zoller, OpenLoops 2, Eur. Phys. J. C **79**, 866 (2019).

[58] S. Actis, A. Denner, L. Hofer, J.-N. Lang, A. Scharf, and S. Uccirati, Recola: REcursive computation of one-loop amplitudes, Comput. Phys. Commun. **214**, 140 (2017).

[59] A. Denner, J.-N. Lang, and S. Uccirati, Recola2: REcursive computation of one-loop amplitudes 2, Comput. Phys. Commun. **224**, 346 (2018).

[60] S. Iguro, T. Kitahara, Y. Omura, and H. Zhang, Chasing the two-Higgs doublet model in the di-Higgs boson production, Phys. Rev. D **107**, 075017 (2023).

[61] S. Frixione, Z. Kunszt, and A. Signer, Three jet cross-sections to next-to-leading order, Nucl. Phys. **B467**, 399 (1996).

[62] A. Denner, S. Dittmaier, M. Roth, and L. H. Wieders, Electroweak corrections to charged-current $e^+e^- \to 4$ fermion processes: Technical details and further results, Nucl. Phys. **B724**, 247 (2005); **B854**, 504(E) (2012).

[63] M. Cacciari, A. Deandrea, G. Montagna, and O. Nicrosini, QED structure functions: A systematic approach, Europhys. Lett. **17**, 123 (1992).

[64] M. Skrzypek and S. Jadach, Exact and approximate solutions for the electron nonsinglet structure function in QED, Z. Phys. C **49**, 577 (1991).

[65] M. Skrzypek, Leading logarithmic calculations of QED corrections at LEP, Acta Phys. Pol. B **23**, 135 (1992), https://www.actaphys.uj.edu.pl/R/23/2/135.

[66] S. Kanemura, Y. Okada, E. Senaha, and C. P. Yuan, Higgs coupling constants as a probe of new physics, Phys. Rev. D **70**, 115002 (2004).

[67] M. Krause, R. Lorenz, M. Muhlleitner, R. Santos, and H. Ziesche, Gauge-independent renormalization of the 2-Higgs-doublet model, J. High Energy Phys. 09 (2016) 143.

[68] L. Altenkamp, S. Dittmaier, and H. Rzehak, Renormalization schemes for the two-Higgs-doublet model and applications to $h \to WW/ZZ \to 4$ fermions, J. High Energy Phys. 09 (2017) 134.

[69] A. Denner, S. Dittmaier, S. Kallweit, and A. Mück, HAWK 2.0: A Monte Carlo program for Higgs production in vector-boson fusion and Higgs strahlung at hadron colliders, Comput. Phys. Commun. **195**, 161 (2015).

[70] S. Brass, W. Kilian, and J. Reuter, Parallel adaptive Monte Carlo integration with the event generator Whizard, Eur. Phys. J. C **79**, 344 (2019).

[71] B. Chokoufe Nejad, T. Ohl, and J. Reuter, Simple, parallel virtual machines for extreme computations, Comput. Phys. Commun. **196**, 58 (2015).

[72] H. Bahl, T. Biekötter, S. Heinemeyer, C. Li, S. Paasch, G. Weiglein, and J. Wittbrodt, HiggsTools: BSM scalar phenomenology with new versions of HiggsBounds and HiggsSignals, Comput. Phys. Commun. **291**, 108803 (2023).

[73] R. Coimbra, M. O. P. Sampaio, and R. Santos, ScannerS: Constraining the phase diagram of a complex scalar singlet at the LHC, Eur. Phys. J. C **73**, 2428 (2013).

[74] M. Mühlleitner, M. O. P. Sampaio, R. Santos, and J. Wittbrodt, ScannerS: Parameter scans in extended scalar sectors, Eur. Phys. J. C **82**, 198 (2022).

[75] P. Bechtle, O. Brein, S. Heinemeyer, G. Weiglein, and K. E. Williams, HiggsBounds: Confronting arbitrary Higgs sectors with exclusion bounds from LEP and the tevatron, Comput. Phys. Commun. **181**, 138 (2010).

[76] P. Bechtle, O. Brein, S. Heinemeyer, G. Weiglein, and K. E. Williams, HiggsBounds 2.0.0: Confronting neutral and charged Higgs sector predictions with exclusion bounds from LEP and the Tevatron, Comput. Phys. Commun. **182**, 2605 (2011).

[77] P. Bechtle, O. Brein, S. Heinemeyer, O. Stál, T. Stefaniak, G. Weiglein, and K. E. Williams, HiggsBounds-4: Improved tests of extended Higgs sectors against exclusion bounds from LEP, the tevatron and the LHC, Eur. Phys. J. C **74**, 2693 (2014).

[78] P. Bechtle, D. Dercks, S. Heinemeyer, T. Klingl, T. Stefaniak, G. Weiglein, and J. Wittbrodt, HiggsBounds-5: Testing Higgs sectors in the LHC 13 TeV era, Eur. Phys. J. C **80**, 1211 (2020).

[79] P. Bechtle, S. Heinemeyer, O. Stål, T. Stefaniak, and G. Weiglein, HiggsSignals: Confronting arbitrary Higgs sectors with measurements at the Tevatron and the LHC, Eur. Phys. J. C **74**, 2711 (2014).

[80] P. Bechtle, S. Heinemeyer, T. Klingl, T. Stefaniak, G. Weiglein, and J. Wittbrodt, HiggsSignals-2: Probing new physics with precision Higgs measurements in the LHC 13 TeV era, Eur. Phys. J. C **81**, 145 (2021).

[81] J. Gu, H. Li, Z. Liu, S. Su, and W. Su, Learning from Higgs physics at future Higgs factories, J. High Energy Phys. 12 (2017) 153.

[82] N. Chen, T. Han, S. Li, S. Su, W. Su, and Y. Wu, Type-I 2HDM under the Higgs and electroweak precision measurements, J. High Energy Phys. 08 (2020) 131.

[83] G. C. Branco, P. M. Ferreira, L. Lavoura, M. N. Rebelo, M. Sher, and J. P. Silva, Theory and phenomenology of two-Higgs-doublet models, Phys. Rep. **516**, 1 (2012).